Multi-scale investigation of the heat-induced transformation of starch in model dough and starch systems

Elham Rakhshi [a], Xavier Falourd [b,c], Ruud den Adel [d], John van Duynhoven [d,e], Tiphaine Lucas [a], Corinne Rondeau-Mouro [a,*]

[a] INRAE, UR1466 OPAALE, 17 Avenue de Cucillé, CS 64427, F-35044, Rennes, France
[b] INRAE, UR1268 BIA, F-44316, Nantes, France
[c] INRAE, BIBS Facility, PROBE Infrastructure, F-44316, Nantes, France
[d] Unilever Foods Innovation Centre, Bronland 14, 6708WH, Wageningen, the Netherlands
[e] Wageningen University & Research, Stippeneng 4, 6708WE, Wageningen, the Netherlands

ARTICLE INFO

ABSTRACT

Our study investigated the impacts of starch botanical origin (tapioca *versus* wheat starch) and gluten addition on the water distribution and hydrothermal changes of starch in model dough systems compared to their pure starch counterparts. In it, we employed a combination of time-domain nuclear magnetic resonance (TD-NMR), wide angle X-ray diffraction (WAXD), solid state nuclear magnetic resonance (ssNMR) at variable temperature (VT) and differential scanning calorimetry (DSC) measurements. The results showed that at intermediate hydration levels, water ingress into starch granules, increase in glucan chain mobility, and dissociation of double helices (DH) of amylopectin occurred at lower temperatures than crystallite loss of order and melting. The inhibitory effect of gluten on wheat starch hydrothermal changes was explained by a higher water adsorption capacity of gluten compared to starch at this hydration level (50%, wb). However this effect was shown to be influenced by starch botanical origin, tapioca-based systems showing no hindrance effect of gluten on starch-water interaction. The study also provides additional evidence for the sensitivity and detection scales of the different techniques at 50% water content.

1. Introduction

Bread is a complex food matrix that requires four essential raw materials: wheat flour, salt, yeast, and water (Eliasson & Larsson, 1993). When these ingredients are mixed and then kneaded, proofed, baked, and cooled, a high-quality bread can be obtained (Mills, Wilde, Salt, & Skeggs, 2003). Starch is the main constituent of wheat flour, representing 70–80% of flour mass on a dry basis (Shevkani, Singh, Bajaj, & Kaur, 2017). Deposited as granules, starch consists of the two glucose polymers amylopectin (AP) and amylose (AM), which form alternating semi-crystalline and amorphous regions known as "growth rings". Starch crystallinity is attributed to crystallites comprising double helices (DH) of AP packed in either hexagonal unit cells (B-type polymorphism) or monoclinic unit cells (A-type polymorphism), while amorphous regions are formed by AM chains and branched segments of AP (Bertoft, 2017). The protein source in wheat flour, representing only 8–14% of its dry weight, consists largely of gluten, composed of insoluble glutenins and soluble gliadins which bond together with disulfide bonds (Wieser, 2007). The heat-induced transformation of dough into bread involves the transformation of the two flour major components, starch and gluten. Numerous interdependent molecular mechanisms contribute to these transformations and their understanding is of considerable interest to the improvement and control of bread quality (Grenier, Rondeau-Mouro, Dedey, Morel, & Lucas, 2021; Lagrain, Wilderjans, Glorieux, & Delcour, 2012). In particular, the thermal transitions of starch and gluten in dough are highly dependent on the water accessible to each of them, interactions between them, and other components present in wheat flour such as lipid residues and arabinoxylans (Debet & Gidley, 2007; Gao et al., 2020; Petrofsky & Hoseney, 1995).

The heat-induced transformation of starch in excess water involves water ingress into granules, disruption of their molecular order, dissociation of double helices, crystallite melting, solubilization and an

---

* Corresponding author.
  E-mail address: corinne.rondeau@inrae.fr (C. Rondeau-Mouro).

increase in aqueous phase viscosity. This transformation, which in its entirety is known as the mechanism of gelatinization, is dependent on starch botanical origin as well as available water (Wang & Copeland, 2013). For gluten, heat-induced transition involves the sub-mechanisms of hydrogen bond disruption (denaturation) and the formation of SS bridges, exposing free sulfhydryl (SH) groups of glutenin and gliadin (crosslinks and aggregations) (Lagrain et al., 2012; Morel, Redl, & Guilbert, 2002). Gluten transition can cause its loss of viscoelasticity and water retention capacity (Grenier et al., 2021; Leon, Rosell, & Benedito de Barber, 2003; Martin, Morel, Reau, & Cuq, 2019; Wagner, Morel, Bonicel, & Cuq, 2011).

At higher bread dough hydration levels (45%–60% depending on the recipe (Petrofsky & Hoseney, 1995)), less extensive starch gelatinization is to be expected compared to excess water conditions, and these conditions may alter the molecular mechanisms mentioned above (Jenkins & Donald, 1998; Kovrlija & Rondeau-Mouro, 2017a; Schirmer, Zeller, Krause, Jekle, & Becker, 2014; Wang, Li, Yu, Copeland, & Wang, 2014). Additionally, the replacement of wheat starch by starches from other botanical origins, as yet rarely investigated at the molecular scale, can also influence these molecular mechanisms (Kovrlija, Goubin, & Rondeau-Mouro, 2020; Milde, Ramallo, & Puppo, 2012; Ratnayake & Jackson, 2007). Meanwhile, available water is also affected by the fact that starch granules in bread dough are embedded in the gluten network and are closely and extensively coated by gliadin molecules, potentially inhibiting their access to water, especially during the heating process (Jekle, Mühlberger, & Becker, 2016; Yang et al., 2022). It is worth noting that lipid-starch and lipid-starch-gluten complexes would also impact the above-mentioned mechanisms, although they are rarely discussed in the literature (Debet & Gidley, 2006; Lelièvre & Liu, 1994).

For over a century, numerous techniques have been used by researchers to elucidate the sub-mechanisms involved in starch gelatinization (Hibbard, 1895). The first technique selected for the present study is differential scanning calorimetry (DSC), which measures the thermodynamic properties of starch and shows transition temperatures, disruption of hydrogen bonds, dissolution of amorphous regions, DH dissociations and loss of molecular order or crystallinity (Biliaderis, Maurice, & Vose, 1980; Cooke & Gidley, 1992; Jenkins & Donald, 1998; Kalichevsky, Jaroszkiewicz, Ablett, Blanshard, & Lillford, 1992; Lelièvre & Liu, 1994). In previous studies, the impact of hydration level, starch botanical origin, pressure, and the presence of non-carbohydrate residues has been investigated using this technique (Baks, Bruins, Janssen, & Boom, 2008; BeMiller, 2011; Zhang, Junejo, Zhang, Fu, & Huang, 2022). A further technique, X-ray diffraction, has demonstrated its usefulness in understanding starch granule structure at the molecular and growth ring scales (Jenkins & Donald, 1998). In particular, the wide angle X-ray diffraction (WAXD) method is sensitive to regular packing, allowing starch crystallinity to be determined by detecting perfectly patched double helices in crystallites with three dimensional order (regular molecular arrangements) (Dome, Podgorbunskikh, Bychkov, & Lomovsky, 2020; Frost, Kaminski, Kirwan, Lascaris, & Shanks, 2009; Nara, Mori, & Komiya, 1978; Vermeylen et al., 2006). This technique has performed very well in the detection of changes to starch crystallinity brought about by physical or chemical treatments (Kuang et al., 2017; Singh, Ali, Somashekar, & Mukherjee, 2006; Zhang et al., 2022).

Solid-state NMR (ssNMR) is the third comprehensive technique selected for the present study. Its combination of magic angle spinning (MAS) cross polarization (CP) and direct polarization (DP) can provide valuable information on helical structures, including the relative contents of double helices (DH), single helices, and less structured starch (Paris, Bizot, Emery, Buzare, & Buleon, 1999, 2001). The influence of hydration, starch origin and physical or chemical treatments has previously been investigated using this technique (Atichokudomchai, Varavinit, & Chinachoti, 2004; Huang, Wang, Fan, & Ma, 2022; Mutungi, Passauer, Onyango, Jaros, & Rohm, 2012; Zhong et al., 2021). Last, but far from least, TD-NMR techniques have been chosen to provide evidence for molecular mobility and water distribution in samples, also

probing the packing of protons in the solid phase (Acri et al., 2021; Riley, Nivelle, Ooms, & Delcour, 2022). This technique has proved effective for real-time monitoring of the mobility and structural changes in samples and provides quantitative data on the solid and liquid phases in the samples. The impact of starch botanical origin on water mobility, heat-induced starch transformation and retrogradation of starch matrices at intermediate hydration levels have previously been elucidated using one and two-dimensional TD-NMR methods (T2, T1, T1-T2) (Kovrlija et al., 2020; Kovrlija & Rondeau-Mouro, 2017b).

In the present study, we set out to provide more evidence for the impact of starch botanical origin on the heat-induced transformation of starch at intermediate hydration levels (45%–50%, chosen for practical reasons) using the above four techniques. The loss of molecular order (DSC) crystallite melting and crystallinity loss (WAXD), mobility changes (TD-NMR) and DH% loss (ssNMR) were considered, all of which are key molecular mechanisms influenced by starch botanical origin during model dough and starch system transformation. In order to facilitate these investigations, starch and model dough systems have been considered using relatively pure starch and gluten as raw materials. This approach has previously been adopted in the literature due to the dough matrix complexity (Bosmans et al., 2012; Doona & Baik, 2007; Gao et al., 2020; Kovrlija et al., 2020; Rondeau-Mouro et al., 2015). Tapioca starch (TS) was chosen, due to its widespread availability and expanding applications in the food industry, alongside wheat starch (WS) as the conventional source of starch for bread dough.

2. Materials and methods

2.1. Materials

Samples were prepared using tapioca starch (Belasie, Rennes, France), wheat starch (Sigma-Aldrich, Saint-Quentin-Fallavier, France), wheat gluten (Eurogerm SAS, France) and distilled water. The amylose and amylopectin contents of starch powders, their damaged starch levels and granule sizes were reported in (Rakhshi, Cambert, Diascorn, Lucas, & Rondeau-Mouro, 2022), in which the methods were also presented. Hydration levels were selected carefully on the basis of preparatory experiments before measurements began. A 45% (wet basis, wb) hydration level was chosen for the model starch systems (TS45 and WS45) in order to avoid phase separation between starch and water. For the model dough systems (TSG50 and WSG50), a higher hydration level of close to 50 % was used, to avoid uneven water distribution and inhomogeneities resulting from the high water retention capacity of gluten. The hydrated samples were prepared freshly for each set of measurements by adding distilled water to pre-weighed amounts of powder, taking into account the water content of the powder itself. Sample water content was determined after analysis by weighing the samples before and after drying in an oven (at 103 °C for 24 h). Table 1 shows the detailed composition of samples and the abbreviations used.

Table 1
Composition of samples and water content of constituents used in their preparation.

Abbreviation	Sample	Gluten content (dry basis)	Water content % (wet basis)
GlP	Wheat gluten powder	90%	9.3 ± 0.1
WSP	Wheat starch powder	–	10.9 ± 0.1
TSP	Tapioca starch powder	–	11.3 ± 0 .1
WS45	WSP + water	–	44.6 ± 0.1
TS45	TSP + water	–	44.0 ± 0.5
WSG50	WSP + water + GlP	11%	49.4 ± 0.6
TSG50	TSP + water + GlP	11%	50.1 ± 0.2

2.2. DSC measurements

DSC measurements were performed on the model dough systems (from 20 to 100 °C at a heating rate of 3 °C/min) using a temperature-modulated differential scanning calorimeter Q100 (TM-DSC Q100, TA Instruments) equipped with a cooler system with a 50.0 ml/min flow rate of nitrogen steam. Parameters and procedures are explained in detail in the authors' previous work (Rakhshi et al., 2022) scanned from 20 to 100 °C.

2.3. WAXD measurements

Wide Angle X-ray diffraction (WAXD) analysis was performed on a Bruker D8-Discover diffractometer in a θ/θ configuration with a Våntec 500 2D detector and an IμS microfocus X-ray source (CuKα radiation, λ = 0.154184 nm). Samples (model dough and starch systems) were placed on an aluminum sample holder using a spatula and their surface was flattened with a cover glass. Samples were covered with Mylar film (heat resistant PET, thickness: 2.5 μm, thin-film width: 76.2 mm, Chemplex Industries inc.), and the Mylar film was then attached to the aluminum sample holder using plastic strips to avoid water evaporation during measurements. A modified Linkam stage (THMS600, Linkam Scientific Instruments, Tadworth, KT20 5LR, United Kingdom) was used to adjust the temperature of the sample holder to 20, 40, 50, 60, 65, 75 and 85 °C. Samples were held at each temperature level for 10 min after stabilization and measurements were then performed, taking10 to 12 min. The sample-to-detector distance was 32.5 cm. The angle of the incident X-ray beam and the sample was 7° and the angles between the detector and the sample were 10°, 25° and 40° respectively, allowing the collection of WAXD data in the range of 7°–55° 2θ.

DIFFRAC.EVA software from Bruker was used for data acquisition and processing. Amorphous phase levels (Amorphous %) and the relative crystallinity percentage (RC%) were calculated using Eq. (1) and Eq. (2) by estimating the global and reduced areas. Background subtraction with an enhanced curvature and threshold equal to 1 allowed the separation of the global and reduced areas, while the crystallinity error that resulted from the Mylar film was corrected using a second background subtraction. The RC% loss between two different temperature levels (from A°C to B°C) was calculated using eq. (3).

$$\text{Amorphous \%} = \frac{\text{Global area - Reduced area}}{\text{Global area}} \times 100 \qquad \text{Eq.1}$$

$$\text{RC\%} = 100 - \text{Amorphous\%} \qquad \text{Eq.2}$$

$$\text{RC\% loss} = \text{RC\% at A °C} - \text{RC\% at B °C} \qquad \text{Eq.3}$$

Dynamic measurements were performed with one replicate. However, in order to obtain valid standard deviations (SD), one matrix was prepared in duplicate and all measurements and data processing were repeated. Maximum SD values (2 %) were extrapolated for the other matrices and used in the plots obtained from WAXD measurements.

2.4. Solid-state NMR (ssNMR) measurements

ss-NMR spectra were registered on a Bruker Advance III 400 spectrometer at a proton frequency of 400.13 MHz and a carbon frequency of 100.62 MHz. ssNMR measurements were performed on model dough and starch systems (one replicate) using both ^{13}C CP-MAS (Cross Polarization – Magic Angle Spinning) and DP-MAS (Direct Polarization) experiments starting at 20 °C and then heating to 40, 60 and 75 °C (decoupling power, 86 W). Temperature calibration was performed using the ^{1}H chemical shift difference for ethylene glycol (Raiford, Fisk, & Becker, 1979). ^{13}C Chemical shifts were calibrated using glycine as the external reference, assigning the carbonyl at 176.03 ppm. For each temperature, the tuning and matching were adjusted and magnetic field homogeneity was improved as far as possible. The spinning rate was set at 9000 Hz. The chronology was as follows: 30 min of holding time at desired temperature, 25 min for CP-MAS acquisition and 35 min for DP-MAS acquisition. For CP-MAS, a contact time of 1.5 ms, 512 accumulations and a 3 s recycling delay were used. The experiments used a 90° proton pulse of 3 μs. For DP-MAS, 2048 accumulations and a 1s recycling delay were selected. The experiments used a 90° carbon pulse of 4.5 μs.

NMR spectra deconvolution was performed using the PeakFit® software (Systat Software, Inc., US). Peak chemical shift and relative contribution were assigned using the method described by Tan & al (Tan, Flanagan, Halley, Whittaker, & Gidley, 2007). DH content was calculated using the C1 peak area measured in CP-MAS spectra. As Fig. 1 shows, to calculate a DH proportion (DH%), the C1 cluster peak areas associated with the double helices (98.2, 99.4 and 100.4 ppm) were divided by the total C1 signal area of the glucose (Paris, Bizot, Emery, Buzaré, & Buléon, 2001). The standard error was assumed to be 2%, based on the literature (Paris et al., 2001).

2.5. TD-NMR measurements

TD-NMR measurements were performed on model dough systems in triplicate (TSG50 and WSG50) using a minispec 20-MHz Bruker spectrometer (Wissembourg, France). T1 (Supplementary Materials, Fig. 13) and T2 relaxation measurements were performed at 20, 40, 50, 60, 65, 75 and 85 °C in all samples after 10 min holding time at the desired temperature, applying a temperature change protocol of 0.2 °C/min as described elsewhere (Rakhshi et al., 2022). The fitting of FID-CPMG signals required the combination of one Gaussian and three exponential functions for all temperatures and was performed using both discrete and continuous methods (TableCurve software and Emilio-FID software©, respectively). Inversion recovery data were processed by the Marquardt method using one or two exponential functions depending on the temperature. The percentage of the solid phase signal proportion (SPH%) was calculated by dividing the sum of the mass intensities (MI) of the first and second T2 components by total sample MI as shown in Eq. (4).

$$\text{SPH\%} = \frac{\text{MI}(1) + \text{MI}(2)}{\text{MI(total)}} \times 100 \qquad \text{Eq.4}$$

2.6. Statistical analysis

Statistical tests were carried out using Statgraphics (Centurion XVI) software. One-way analysis of variance made it possible to detect any

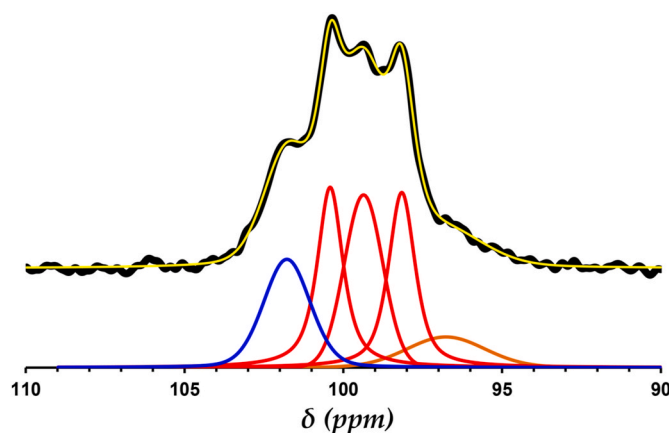**Fig. 1.** Deconvolution of the ^{13}C CPMAS spectrum C1 region of WS45. Black line corresponds to experimental data, yellow line corresponds to the sum of individual peaks resulting from the spectral deconvolution. The blue peak (101.8 ppm) is assigned to single helices, red peaks (98.2, 99.4 and 100.4 ppm) are assigned to DH and the orange peak to less structured starch.

significant differences (95% confidence) between NMR parameters (T2 or MI values) at different temperatures (groups designated by letters a–f).

3. Results

3.1. DSC measurements

The thermal properties of the samples under study were investigated using DSC measurements. As shown in Table 2, two endotherms were quantified for all systems at a temperature range of approximately 50–100 °C. In general, higher gelatinization enthalpies (ΔH 1) and lower onset and peak gelatinization temperatures (To, Tp 1 and Tp 2) were observed for WS-based matrices compared to TS ones. In starch systems, ΔH 1+ΔH 2 (or ΔH 1'+ΔH 2' expressed in mass of dry starch) and ΔH 2 values were higher for WS45 than for TS45, while in model dough systems these values were lower for WSG50 than TSG50. Moreover, higher gelatinization enthalpies and lower Tp 2 values were observed for both model dough systems compared to the starch systems. To and Tp1, Tc values remained constant for TS-based matrices when comparing model dough systems to starch systems, while WSG50 displayed lower values compared to WS45 for these parameters.

3.2. WAXD diffractograms

The diffractograms of starch powders WSP and TSP at 20 °C are shown in Fig. 2. Due to the semi-crystalline nature of starch granules, broad diffraction peaks and a large amorphous area were observed. Peaks at around 15°, 17°, 18° and 23° were detected for both WSP and TSP (shown by vertical lines in Fig. 2). Fig. 3 presents the diffractograms obtained for TS45, WS45, TSG50 and WSG50 at different temperatures (from 20 to 85 °C). The diffraction peaks were the same as those identified for WSP and TSP. It was also shown that the intensity of these peaks became gradually weaker as the temperature increased. Additionally, RC% evolution as a function of temperature for all systems is shown in Fig. 4. At 20 °C, a higher RC% was observed for TS systems than for WS systems (20% vs 15% for TS45 compared to WS45, and 18% vs 13% for TSG50 compared to WSG50). Temperature increases below the To obtained by DSC for these systems (Table 2) produced no significant changes (showed by black arrows), while above the To, a decreasing trend was observed for all matrices (Fig. 4). By selecting 60 °C as the approximate intermediate point between all To values (in all systems), it was possible to calculate the RC% loss as shown in Fig. 5. Here, the above trend is strongly confirmed and, above 60 °C, a greater RC% loss can be observed for TS45 compared to the other systems.

3.3. ^{13}C CP-MAS and DP-MAS analysis

Fig. 6 shows the ^{13}C CP-MAS and DP-MAS spectra obtained for the different matrices at 20 °C. Differences were observed between TS and WS matrices as well as between model dough and starch systems. As can be seen, the addition of gluten and 5% water modified the starch local

structure and/or mobility at 20 °C, with visible changes in the most mobile parts of the AM and AP chains observable on the ^{13}C DP-MAS spectra. Indeed, in the case of WSG50, we observed a peak around 77 ppm (marked with an asterisk, Fig. 6b), that could be assigned to the C4 of AM single helices. For the rigid parts of the chains evidenced by CP-MAS (Fig. 6a), the addition of gluten and 5% water does not lead to major changes in the spectra. Increasing temperature induced changes in the CP-MAS spectra, in particular in the C1 peak for starch. Changes in the double helix proportion calculated from C1 peaks (DH%) were calculated at different temperatures and are plotted in Fig. 7. At 20 °C, TS-based systems displayed higher DH% values (79% vs 73% for TS45 compared to WS45 and 75% vs 65% for TSG50 compared to WSG50). Moreover, both model dough systems displayed lower DH% compared to their model starch counterparts (regardless of starch origin). To aid the discussion, DH% loss across the different temperature intervals was also calculated (Fig. 8). With heating, a decreasing trend in DH% was observed for all matrices. More precisely, at temperatures below 60 °C, DH loss was dominant and higher for model starch systems (solid columns in Fig. 8) compared to model dough systems (hatched columns in Fig. 8), but this difference vanished between 60 °C and 75 °C (taking the standard errors into account). The values calculated in this temperature range were not dramatically different in the model dough matrices regardless of starch origin, and a smaller loss was observed above 60 °C in the model starch systems. No significant difference was observed between 60 °C and 75 °C for WS-based systems while the loss observed for TSG50 was higher than that for TS45. In general, from 20 to 75 °C, WSG50 displayed a higher DH loss than TSG50. In addition, a higher DH loss was observed in model starch systems (solid columns in Fig. 8) compared to model dough systems (hatched columns in Fig. 8), regardless of starch origin.

3.4. TD-NMR measurements

Table 3 shows the T2 relaxation times and their MI obtained by TD-NMR measurements for WSG50 and TSG50 at different temperatures. As is shown, four different components were distinguished for both matrices at 20 °C (T2 (1), T2 (2), T2 (3) and T2 (4)). At 20 °C, significant differences could be observed between T2 (2) and T2 (4) values (56.3 μs vs 65.1 μs and 18.9 ms vs 28.2 ms for TSG50 and WSG50 respectively). With the increase in temperature, the number of components remained constant but changes in T2 values and MI were noted and confirmed by statistical analysis (indicated by letters in Table 3). The standard deviations for the evolutions of T2 relaxation times in these two matrices were generally quite similar (see Supplementary Materials to compare detailed values for the model starch and dough matrices, Fig. 14, 15 and 17). However, their MI evolutions displayed significant differences, as plotted in Fig. 9. MI(1) showed a decreasing trend for both matrices, which is consistent with Curie's law on the effect of temperature. By contrast, variations in MI(2) suggested differences in the behaviour of these two matrices. For TSG50, MI(2) remained quite constant, while for WSG50, a slight increase was observed from 20 to 50 °C followed by a decreasing trend above this temperature. MI(3) values obtained for

Table 2
Onset temperature (To), peak temperatures (Tp 1 and Tp 2) for the first (P1) and second (P2) endotherms respectively, conclusion temperature (Tc), associated gelatinization enthalpies (ΔH 1 and ΔH 2) and their sum (ΔH 1 + ΔH 2) or (ΔH 1'+ΔH 2') given as mean ± standard deviation values. (ΔH 1 + ΔH 2) and (ΔH 1'+ΔH 2') are expressed in gram of hydrated matrix or in gram of dry starch, respectively.

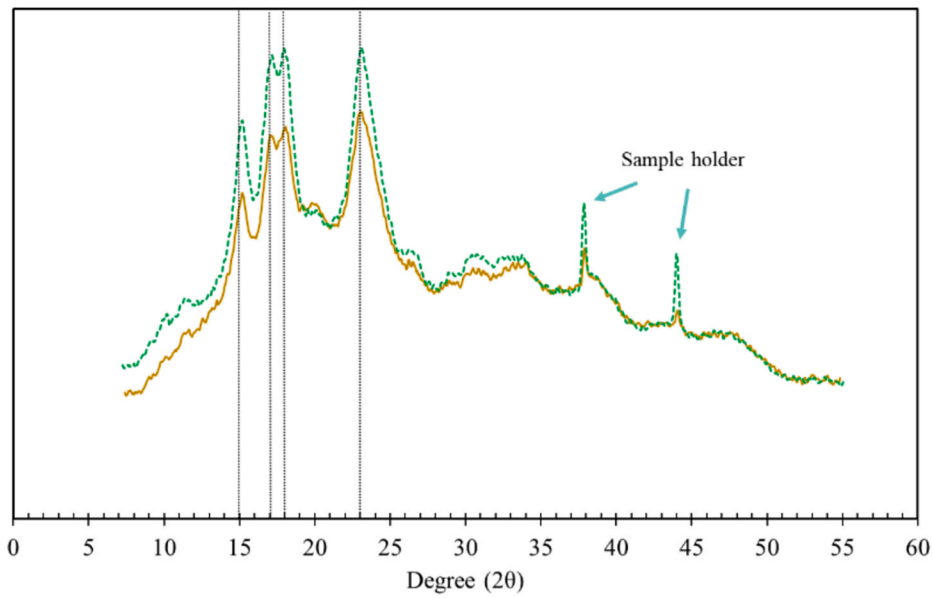| Sample	To (°C)	Tp 1 (°C)	ΔH 1 (J/g)	Tp 2 (°C)	Tc (°C)	ΔH 2 (J/g)	ΔH 1+ΔH 2 (J/g)	ΔH 1'+ΔH 2' (J/g)
WSG50	53.4	57.9	12.5	82.4	93.0	3.4	15.9	35.8
	±0.1	±0.2	±1.1	±0.7	±0.1	±0.2	±1.3	±2.9
TSG50	63.1	67.3	8.1	92.2	103.1	10.9	18.9	42.5
	±0.1	±0.1	±1.0	±0.1	±1.1	±0.1	±1.0	±2.2
WS45	56.4	61.4	3.0	85.1	99.8	2.1	5.1	9.3
	±0.1	±0.2	±0.2	±0.3	±0.5	±0.6	±0.8	±0.8
TS45	62.8	67.2	1.8	94.1	103.6	1.0	2.8	5.1
	±0.1	±0.1	±0.2	±0.4	±2.1	±0.1	±0.2	±0.4

Fig. 2. Wide-angle X-ray diffraction patterns for WSP (solid line) and TSP (dotted line) at 20 °C.
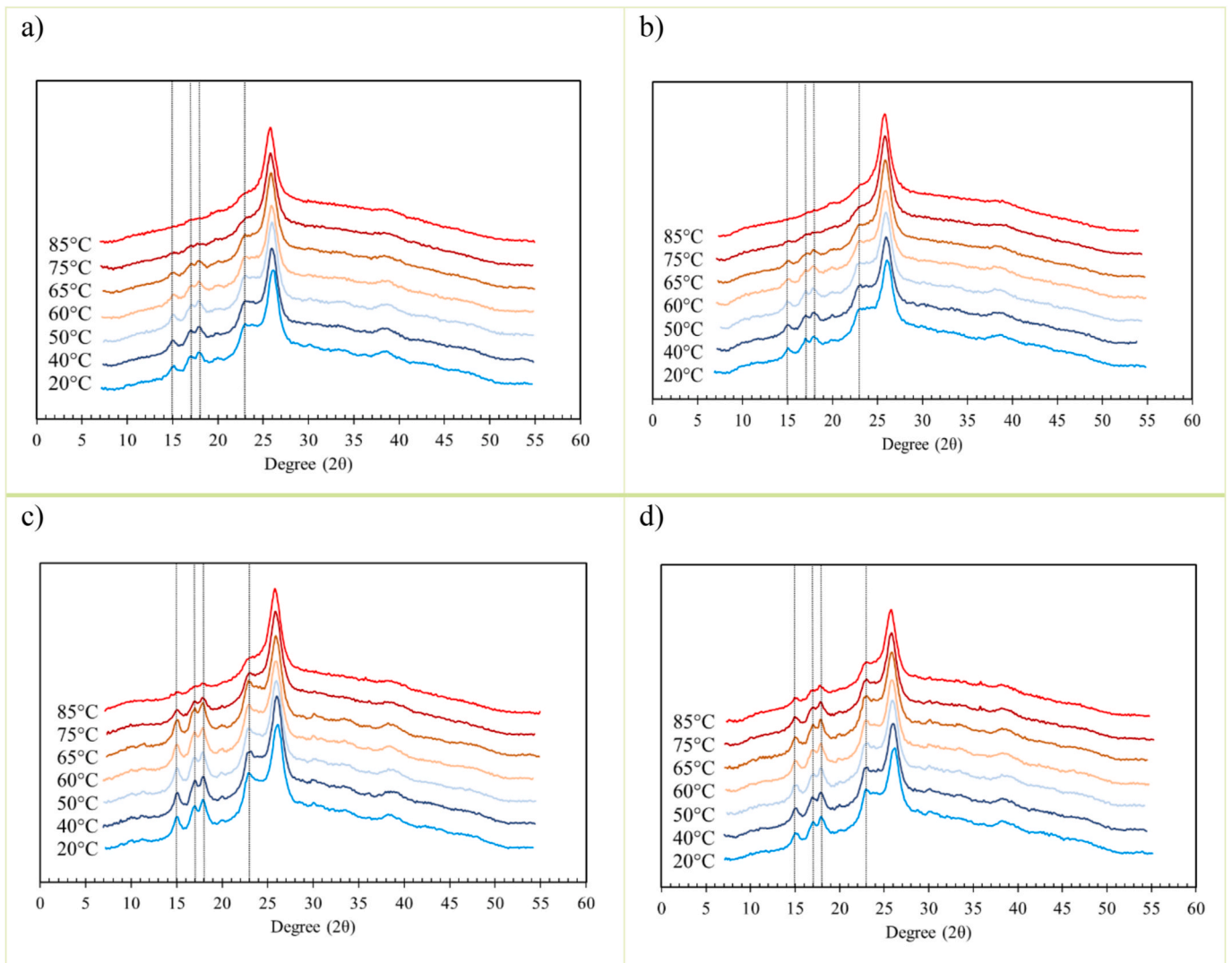

Fig. 3. Wide-angle X-ray diffraction patterns for WS45 (a), WSG50 (b), TS45 (c), TSG50 (d) as a function of temperature (20–85 °C). The high-intensity peak at 26° is produced by the Mylar film used to avoid water evaporation from the samples.
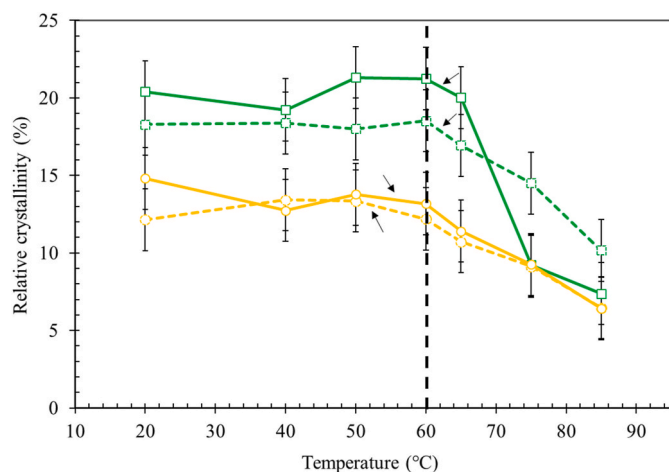
Fig. 4. RC percentage (RC%) obtained for starch (solid lines) and model dough (dotted lines) systems. Systems based on TS are shown by squares (green) while WS-based systems are designated by circles (yellow). The To, as obtained with DSC, is indicated by a black arrow for each system. The dotted vertical bar at 60 °C indicated the approximate intermediate temperature between all To values (in all systems).

TSG50 remained constant from 20 to 50 °C and then slightly increased from 50 to 60 °C. Above 60 °C, a slight decrease was observed, consistent with Curie's law. For WSG50, MI(3) remained constant from 20 to 40 °C, before increasing slightly from 40 to 50 °C. From 50 to 65 °C, it remained constant and then decreased above 65 °C. MI(4) values remained constant for WSG45 and a decrease was observed from 50 to 60 °C for TSG50. This decrease was followed by an increase from 65 to 85 °C.

In order to investigate the evolution of MI in solid and liquid phase T2 components, the percentage of the solid phase signal (SPH%) was calculated (according to Eq. (4) given in the Materials & Methods section) which took Curie's law into account. Fig. 10 shows the evolutions of SPH% for the model dough systems in the present study and starch systems studied in our previous work (Rakhshi et al., 2022). At all temperatures, slightly higher values were observed for TS-based systems. A decrease in SPH% was observed immediately above the To,

marking a change from the constant trend observed below To for these systems (To indicated by black arrows in Fig. 10). The SPH% losses below and above 60 °C and from 20 to 85 °C are shown in Fig. 11. Below 60 °C, WS-based systems showed a slightly higher SPH% loss, while no significant difference in standard error was observed between model dough and starch systems. Above 60 °C, TS-based matrices showed higher SPH% loss, again with no significant difference between the model dough and starch systems. From 20 to 85 °C, the same trends as for 20–60 °C were observed for these four systems.

4. Discussion

4.1. Transition temperatures and enthalpies

Comparison of gelatinization parameters obtained by DSC measurements for TS45 and WS45 has been discussed extensively in our previous work (Rakhshi et al., 2022). In the present work, we used exactly the same raw materials. In brief, we found starch botanical origin to significantly impact DSC parameters due to differences in AM/AP ratio, AP organization at molecular scale, damaged starch levels and presence of non-carbohydrate residues. The higher To, Tp1 and Tp2 observed for TS45 compared to WS45 were attributed to TS45's lower amylose/amylopectin ratio (0.24 vs 0.40), lower level of damaged starch (<0.3 vs 1.1 %) and tighter crystallite organization (values from Table 2 in Rakhshi et al., 2022). Globally, the lower gelatinization enthalpy observed for TS45 compared to WS45 was attributed to its more stable structure, meaning that it would require more water to lose its order (Bertoft, 2017; Rakhshi et al., 2022). DSC parameters obtained for model dough systems showed higher To, Tp1, Tp2 and Tc values for TSG50 compared to WSG50, which was in line with results obtained for starch systems, and for these starches in excess water conditions (Rakhshi et al., 2022). These results highlight the role of starch botanical origin in starch transition temperatures. ΔH 1, indicating the plasticization of amorphous regions and DH dissociations, was higher for WSG50 than for TSG50 (Waigh, Gidley, Komanshek, & Donald, 2000). On the other hand, ΔH 2, assigned to helix-coil transitions, showed an opposite trend to ΔH 1 (Waigh et al., 2000). We should remember that TS45 values for both ΔH 1 and ΔH 2 were lower than those for WS45, which may suggest a more compact organization (thinner amorphous lamella) and lower DH dissociations during gelatinization (Vamadevan
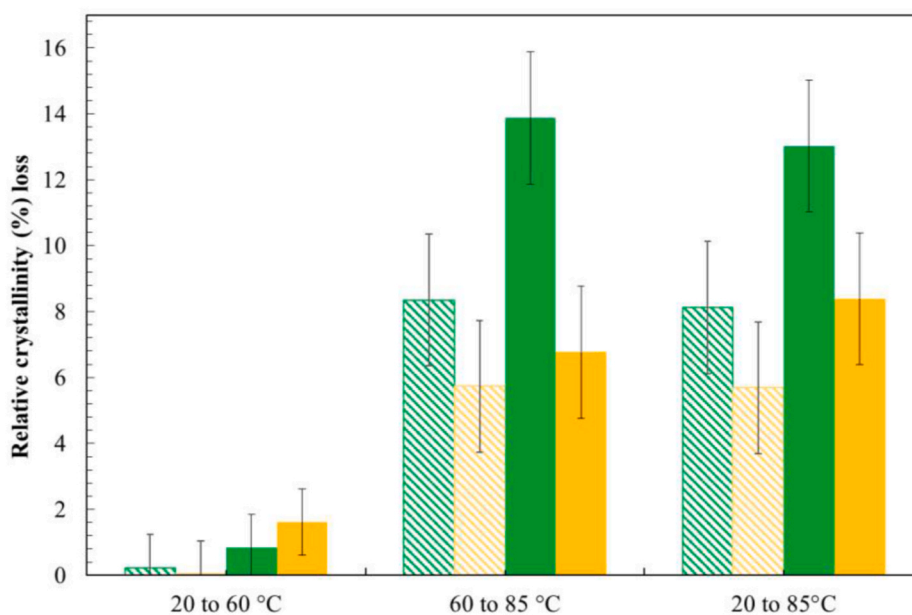

Fig. 5. RC% loss for different temperature intervals for WS45 (solid yellow columns), TS45 (solid green columns), WSG50 (hatched yellow columns) and TSG50 (hatched green columns).
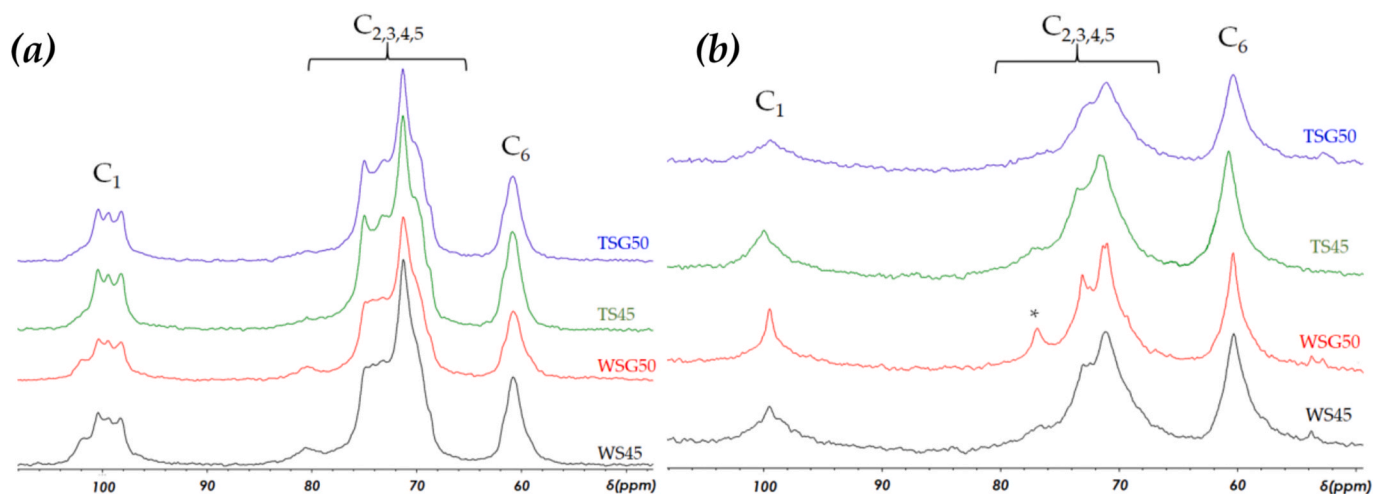
Fig. 6. a) ^{13}C CP-MAS and (b) DP-MAS spectra obtained for the different systems at 20 °C. The asterisk in Fig. 6b (at 77 ppm) is likely to represent the C4 of AM single helices in WSG50.
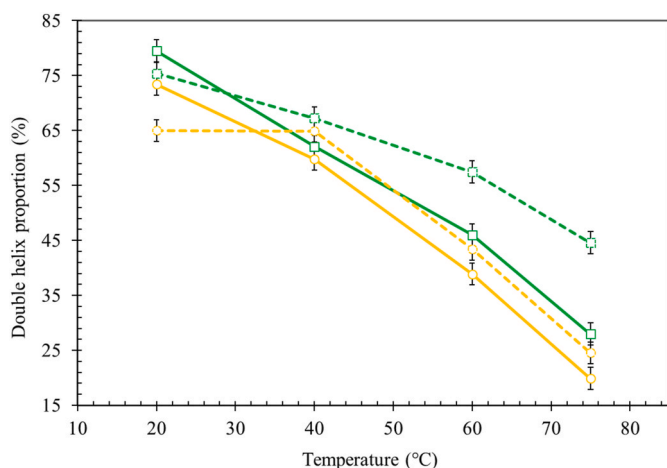

Fig. 7. Double helix proportion (DH%) obtained for starch systems (solid lines) and model dough systems (dotted lines). TS-based systems are represented by squares (green), while WS-based systems are represented by circles (yellow). The standard error was assumed to be 2% based on the literature (Paris et al., 2001).
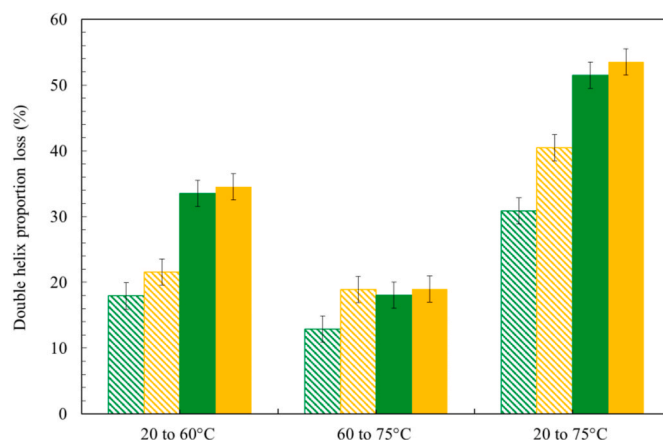

Fig. 8. Double helix proportion loss (in percentage %) obtained for different temperature ranges from WS45 (solid columns in yellow), TS45 (solid columns in green), WSG50 (hatched columns in yellow) and TSG50 (hatched columns in green). The standard error was assumed to be 2% based on the literature (Paris et al., 2001).

& Bertoft, 2020). These observations confirm the determining influence of hydration levels on starch transition enthalpies already suggested in the literature (Baks et al., 2008; Eliasson, 1980). The 5% increase in hydration level and addition of gluten contributed to the higher ΔH2 for TSG50 compared to WSG50. This may indicate that loss of order occurs at higher temperatures for TSG50 than for WSG50. This suggestion is in line with the retarded but more intense gelatinization of TS compared to WS in excess water (pure starch systems) reported in the literature (Debet & Gidley, 2006). In terms of transition temperatures (To, Tp and Tc), it can be suggested that TS showed less dependency on hydration level and gluten addition than WS (comparing model dough systems to starch systems). However, these observations could not be used for a full assessment of the inhibitory effect of gluten on starch gelatinization proposed by the literature, due the different hydration level and high heating rate applied for these measurements (3 °C/min) in the present study. It should be emphasized that only the parameters obtained from 20 to 85 °C were useful to the discussion of other results in this work (To, Tp and ΔH 1).

4.2. Relative crystallinity (RC%)

The diffraction lines observed for WSP and TSP (15°, 17°, 18° and 23°) provide evidence to support the crystallinity types proposed for TS and WS in the literature (cereal vs root family) (Singh et al., 2006) (Fig. 2). It is widely believed that WS belongs to the group of starches characterized by A-type polymorphs while TS belongs to the C-type polymorph group combining both A- and B-type polymorphs. Since TSP includes both A and B-types, its diffractogram could be expected to show similarities to that of WSP. The peaks detected close to 15°, 17°, 18° and 23° corresponded quite well to the description of AP crystallites in the literature for these two starch types (Dome et al., 2020; Singh et al., 2006).

The diffraction lines in the WAXD diffractograms obtained for model dough and starch systems gradually decreased in intensity as temperature increased, indicating crystallite loss of order as the result of heating and the diffusion of water into the semi-crystalline starch lamella (Fig. 3). At 20 °C, the higher RC% observed for TS45 compared to WS45 (20 vs 15%, Fig. 4) was in line with previous findings using the same technique: Singh et al. reported RC% values of 35 and 28 % for TSP and WSP (12.5% w. b) respectively, in line with the present results for differences in hydration levels (Singh et al., 2006). Below 60 °C, RC% loss

Table 3
Mean values and standard deviations of T2 relaxation times (ms or μs) and mass intensities (MI (V/g)) for TSG50 and WSG50. Numbers refer to the different components and letters designate the results of statistical analysis (ANOVA).

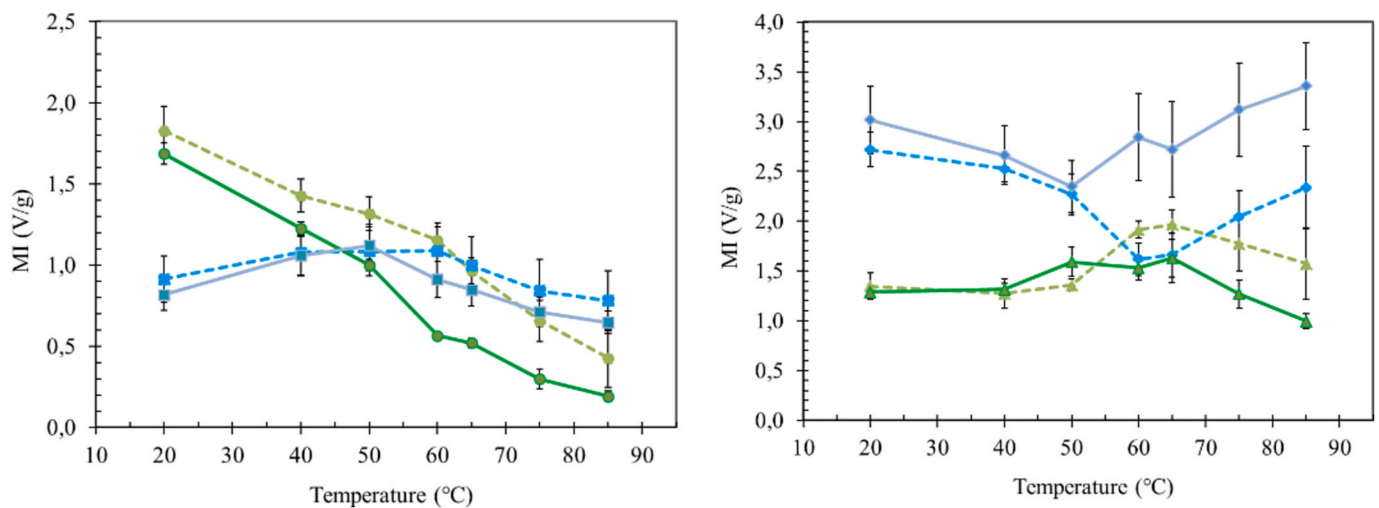| Sample	Temp (°C)	T2(1) (μs)		MI(1) (V/g)		T2(2) (μs)		MI(2) (V/g)		T2(3) (ms)		MI(3) (V/g)		T2(4) (ms)		MI(4) (V/g)	
TSG50	20	18.4 ± 0.1	a	1.83 ± 0.15	a	56.3 ± 2.7	a	0.91 ± 0.14	ab	2.8 ± 0.1	a	1.35 ± 0.13	a	18.9 ± 1.7	a	2.72 ± 0.18	a
TSG50	40	18.2 ± 0.2	a	1.43 ± 0.1	b	66.1 ± 6.1	ab	1.08 ± 0.14	b	2.8 ± 0.5	a	1.27 ± 0.15	a	15.3 ± 1.5	bc	2.53 ± 0.14	ab
TSG50	50	18.2 ± 0.3	a	1.32 ± 0.11	bc	78 ± 6	bc	1.09 ± 0.15	b	3 ± 0.6	a	1.36 ± 0.06	a	13.8 ± 1.1	c	2.27 ± 0.21	bc
TSG50	60	18.2 ± 0.3	a	1.15 ± 0.08	cd	96.9 ± 6.9	cd	1.09 ± 0.17	b	3.9 ± 0.2	bc	1.91 ± 0.09	bc	14.2 ± 0.9	bc	1.62 ± 0.16	d
TSG50	65	18.3 ± 0.5	a	0.96 ± 0.08	d	105 ± 8.6	d	1 ± 0.17	ab	4.1 ± 0.1	bc	1.96 ± 0.15	c	16.2 ± 0.7	b	1.66 ± 0.22	d
TSG50	75	17.8 ± 1.1	a	0.66 ± 0.13	e	117.5 ± 15.3	de	0.84 ± 0.19	ab	4.4 ± 0.4	bc	1.77 ± 0.27	bc	16 ± 1	bc	2.04 ± 0.27	cd
TSG50	85	16.9 ± 2.1	a	0.43 ± 0.18	f	134.6 ± 20.8	e	0.78 ± 0.19	a	4.9 ± 0.6	c	1.57 ± 0.36	ab	19.9 ± 1.7	a	2.34 ± 0.41	abc
WSG50	20	18.7 ± 0.1	a	1.69 ± 0.06	a	65.1 ± 2.8	a	0.82 ± 0.09	ab	3.2 ± 0.1	a	1.29 ± 0.07	a	28.2 ± 3.4	a	3.02 ± 0.34	ab
WSG50	40	18.8 ± 0.4	a	1.23 ± 0.04	b	73.8 ± 2.1	a	1.06 ± 0.12	cd	3.7 ± 0.2	ab	1.31 ± 0.06	ac	23 ± 2.4	bc	2.66 ± 0.29	ab
WSG50	50	18.4 ± 0.3	ab	1 ± 0.04	c	90.6 ± 3.4	b	1.12 ± 0.13	d	4.6 ± 0.2	bc	1.59 ± 0.14	b	18.5 ± 2.5	cd	2.35 ± 0.26	b
WSG50	60	16.8 ± 1.3	ab	0.57 ± 0.01	d	103.7 ± 8.9	c	0.91 ± 0.11	bc	5.1 ± 0.5	c	1.53 ± 0.12	bc	14.2 ± 1.2	d	2.84 ± 0.44	ab
WSG50	65	16.6 ± 1.1	ab	0.52 ± 0.03	d	109.2 ± 8.6	c	0.85 ± 0.1	ab	5.3 ± 0.8	c	1.63 ± 0.25	c	14.3 ± 1.5	d	2.72 ± 0.48	ab
WSG50	75	16.4 ± 2	bc	0.3 ± 0.06	e	128.7 ± 11.1	d	0.71 ± 0.09	ae	5.7 ± 1.2	c	1.27 ± 0.14	a	18.4 ± 3.3	cd	3.12 ± 0.47	a
WSG50	85	16 ± 2.2	c	0.18 ± 0.03	f	127.7 ± 3	d	0.63 ± 0.07	e	5.7 ± 0.7	c	1 ± 0.09	d	27.7 ± 3.9	ab	3.33 ± 0.53	a

Fig. 9. MI(1), MI(2), MI(3) and MI(4) designated by circles, squares, triangles and diamonds respectively for WSG50 (solid lines) and TSG50 (dotted lines) as a function of temperature.

was negligible and quite similar in TS45 and WS45 (Fig. 5), as can be expected given that crystallite melting has already been observed to be non-existent or very limited under these conditions (Jenkins & Donald, 1998). Above 60 °C, a higher RC% loss was observed than below 60 °C, which can be explained by the dependency of crystallite melting on temperature (the To of these systems is indicated by black arrows, Fig. 4). It can be deduced that crystallite melting occurred only above To in these systems. The later RC% loss for TS45 compared to WS45 could be explained by the former's higher Tp 1, Tp 2 and Tc. Overall RC% loss (20–85 °C) was higher for TS45 compared to WS45, a result that was not consistent with its lower ΔH 1 obtained by DSC measurements (Table 2). This may be due to the lower sensitivity of the WAXD technique to changes occurring at molecular scale.

As with the starch systems, the RC% obtained by WAXD measurements in model dough systems started to decrease above To and the RC% loss observed from 20 to 60 °C was negligible (Figs. 4 and 5). A lower initial RC% in model dough systems compared to starch systems can be attributed to the higher hydration level and the effect on their diffractograms of the presence of gluten amorphous areas. Above 60 °C (as for the 20–85 °C temperature range), RC% loss was similar for TSG50 and WSG50, in line with the relatively close ΔH 1 values observed for the two systems (12.5 ± 1.1 vs 8.1 ± 1.0 J/g for WSG50 and TSG50 respectively). Comparison of losses observed for these systems to those obtained for starch systems revealed lower values for TS-based systems (due to the inhibitory effect of gluten addition) despite higher hydration levels, while no significant changes were observed for WS-based
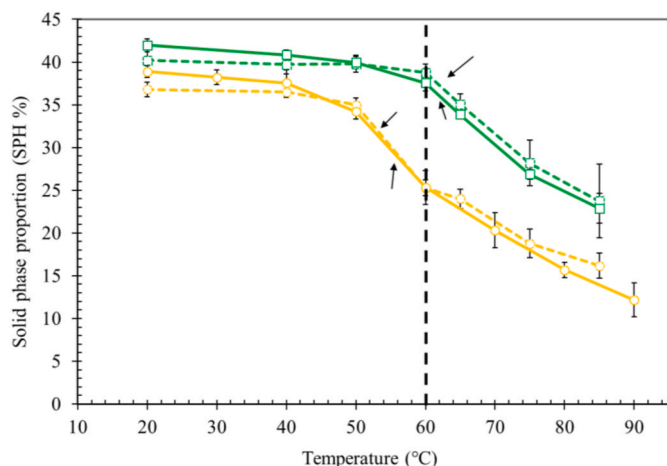
Fig. 10. SPH% values obtained for starch systems (solid lines) and model dough systems (dotted lines). TS-based systems are denoted by squares (green) while WS-based systems are denoted by circles (yellow). Arrows indicate the gelatinization onset temperature (To) for the different systems. The dashed vertical bar marks the transition temperature used to integrate SPH% across different temperature ranges as shown in Fig. 11.

systems. This observation was not in line with the higher ΔH 1 for model dough systems obtained by DSC measurements. The discrepancy can be attributed to the lower sensitivity of WAXD measurements to DH dissociations, the plasticization effect of water and differences in the heating rates used for these matrices.

4.3. Double helix proportion (DH%)

DH% values calculated based on ssNMR measurements at 20 °C showed higher values for TS-based systems, agreeing with the RC% values measured by WAXD already attributed to the higher crystallinity of TS (Fig. 7). The starch systems also showed a higher DH% compared with their model dough counterparts at 20 °C, possibly due to the effects of amorphous gluten addition and lower water availability for starch (hydration levels are known to affect DH content, (Paris et al., 1999,

2001). Below 60 °C, lower DH% loss was observed for model dough systems than for starch systems, which may indicate retarded dissociation of DH in these systems as a result of gluten addition (Fig. 8). However, above 60 °C, similar DH% losses were observed in both model dough and starch systems, which could be attributable to the influence of temperature on DH dissociation. The botanical origin of the starch was observed to have no significant impact (no difference below 60 °C and a slight difference above 60°) on these systems, probably because the DH dissociation was so strongly dependent on hydration level and temperature. Above 60 °C, an inhibitory, "hindrance effect" of gluten addition on TS-based matrices was discernible. From 20 to 75 °C, DH% loss was observed to be higher in WSG50 than in TSG50, which can be attributed to the higher temperatures required for TS to lose its structure. Moreover, in this temperature range, an inhibitory effect of gluten on DH-dissociations could be observed for both TS- and WS-based matrices.

4.4. MI and solid phase proportion (SPH%)

Investigation of MI changes in solid and liquid phase T2 components, produced results, expressed in solid phase proportion (SPH%), that were relatively similar for systems prepared with starch of the same botanical origin (Fig. 10). In other words, the addition of gluten did not impact the evolution of SPH%, in line with previous findings that, in model dough systems, T2 profiles match those in their pure starch counterparts. Indeed, starch molecular dynamics are known to be dominant during dough transformation (Nivelle, Beghin, Bosmans, & Delcour, 2019; Rondeau-Mouro et al., 2015). MI-based calculations that take sample water content and Curie's law into account, would thus appear to offer a reliable comparison of model dough and starch systems, as can be seen from Fig. 10. At 20 °C, the higher SPH% observed for TS-based systems compared to WS-based systems was to be expected, due to the higher AP content and tighter organization of TS (and was also in line with RC% and DH% values). Below 60 °C, a higher SPH% loss was observed for WS-based systems, consistent with the lower To and weaker organization of WS compared to TS (Fig. 11) (Vamadevan & Bertoft, 2015). Above 60 °C, TS-based systems were shown to have higher SPH% losses, again consistent with the higher To in TS. These observations suggest that TD-NMR is highly sensitive to the botanical origin of starch and to its structural changes during hydrothermal transformation, expanding
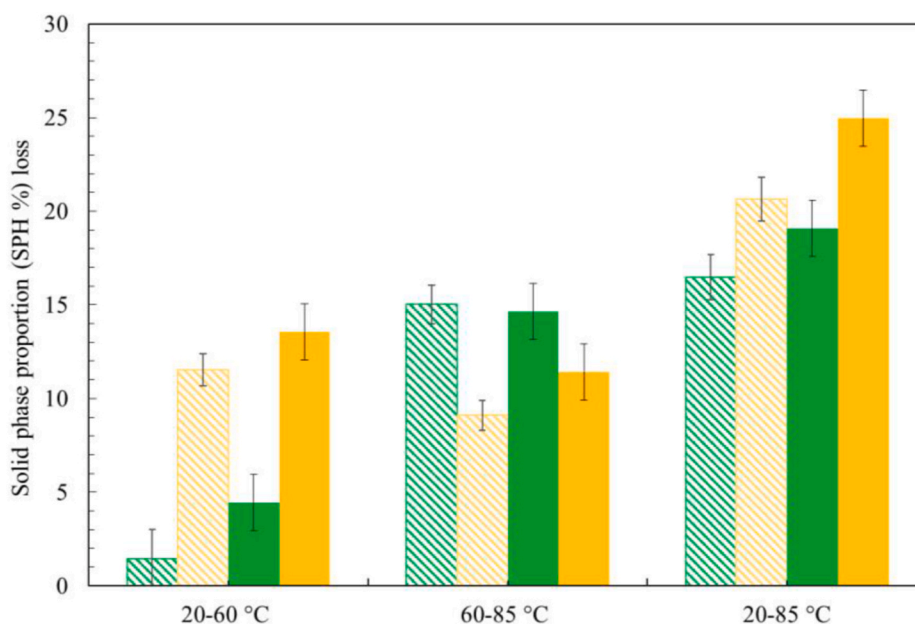

Fig. 11. SPH% loss at different temperature ranges obtained for WS45 (solid columns in yellow), TS45 (solid columns in green), WSG50 (hatched columns in yellow) and TSG50 (hatched columns in green).
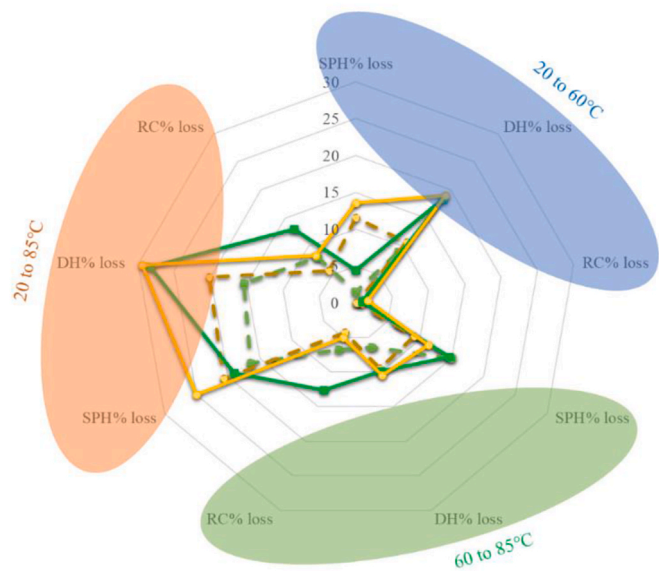
Fig. 12. Comparison of SPH%, DH% and RC% loss at different temperature ranges obtained for model dough systems (dotted lines) and starch systems (solid lines). TS-based systems are shown with square symbols (in green) and WS-based systems shown with circle symbols (in yellow).

on previous claims based on wheat starch alone.

Overall SPH% loss from 20 to 85 °C was higher for WS-based systems, attributable to the known dominant role of starch botanical origin in water absorption and the increased mobility of starch protons. A hindrance effect of gluten on SPH% was observed for WS-based systems, calling into question previous claims in the literature (Bosmans et al., 2012; Rondeau-Mouro et al., 2015). Using the Guggenheim–Anderson–de Boer model, at hydration levels close to those of bread dough, gluten has been shown to have the capacity to absorb water, confirming its inhibitory effect on the access of starch granules to water (Roman-Gutierrez, Guilbert, & Cuq, 2002). Although evidence for this claim has been provided by other techniques, the results of TD-NMR investigations, with the exception of a single work, have never validated this role for gluten (Bosmans et al., 2012). Our observations thus offer the first quantitative result to demonstrate the impact of gluten on dough water distribution, an issue repeatedly debated in the literature (Doona & Baik, 2007; Eliasson, 1983; Riley et al., 2022). Regarding the standard deviations observed for TS45 and TSG50, no hindrance effect of gluten could be observed for the

TS-based systems, raising questions concerning the dependency of dough water distribution on starch origin (TS has a high water absorption capacity) or on starch-gluten interactions that might differ with the starch origin.

4.5. T2 relaxation times and their assignment

T2 relaxation times obtained for the model dough systems in this work were assigned to different proton pools, using a binary model system to achieve greater precision. Table 4 presents the T2 assignments proposed here alongside previous T2 findings put forward by this team (Rondeau-Mouro et al., 2015). Fewer components were identified in the present study compared to those reported by Rondeau-Mouro et al., a fact attributable to differences in sample composition (Rondeau-Mouro et al., 2015). Nevertheless, the T2 (1), T2 (2), T2 (3) values reported in the earlier study were quite similar to T2 values in the present work, as could be expected given the very similar hydration levels.

A comparison of T2 values and their evolution for binary and trinary systems revealed differences, mostly between liquid components, that were attributed to the difference in hydration levels (Supplementary Materials, Figs. 15 and 17). Since T2 relaxation times were strongly dependent on hydration levels, these comparisons were restricted to MI-based calculations (previous section). On the other hand, the difference between T2 (4) values obtained for TSG50 and WSG50 at 20 °C, can be attributed the higher water absorption capacity of TS (due to more starch-water interactions) compared to WS. No significant impact of starch botanical origin on other T2 evolutions or on the number of components was observed (Table 3 and Supplementary Materials, Fig. 14).

4.6. Correlation of multiscale structural features

To better illustrate the correlation between values obtained with different techniques (WAXD, ss-NMR and TD-NMR) and the differences between the four different systems studied, results were represented in form of a spider chart and a table (Fig. 12 and Table 5).

From 20 to 60 °C, RC% loss was negligible compared to the dominant DH% loss and relatively high SPH% loss. This observation suggests that DH dissociations and enhanced starch (and gluten) protons mobility, due to water ingress and plasticizing effect of water, precede crystallites melting.

From 60 to 85 °C (60–75 °C in case of DH% loss), DH% and SPH% loss were quite coherent between almost all systems that can indicate the interdependency of DH dissociations, glucan solubilization and

Table 4

Comparison of T2 components and their assignments proposed for model dough systems with T2 assignments previously proposed in the literature (at 20 °C).

T2 components		Model dough (wheat flour, yeast water, 44% wet basis) Rondeau-Mouro et al. (2015)	Model dough systems (50%, present study)
T2(1)	≈18 μs	Non-exchanging protons from starch in semi-crystalline regions	TSG50: 18.4 ± 0.1 μs WSG50: 18.7 ± 0.1 μs	Non-exchanging protons from starch AP, AM and gluten backbone
T2(2)	≈60 μs	Non-exchanging protons from starch in amorphous regions and gluten chains with little (low) contact to water	TSG50: 56.3 ± 2.7 μs WSG50: 65.1 ± 2.8 μs	Non-exchanging protons from starch in amorphous regions and gluten functional groups with more mobility
T2(3)	≈2.0 ms	Exchanging protons from intra-granular water, starch, gluten and water inside gluten sheets	TSG50: 2.8 ± 0.1 ms WSG50: 1.29 ± 0.07 μs	Exchanging protons from intra-granular water and starch Exchanging protons from confined water and gluten protons
T2 (4)	≈9.7 ms	Exchanging protons from extra-granular water, starch, gluten and water outside gluten sheets	TSG50: 18.9 ± 1.7 ms WSG50: 28.2 ± 3.4 ms	Exchanging protons from water in gluten macropores (in interaction with confined water) and water in indirect exchange with starch (extra-granular water), protons from lipid residues
T2(5)	≈309 ms	Extra-granular water protons exchanging with other water fractions	N.D	–

Table 5

Comparison of starch and model dough systems using different parameters obtained from DSC, WAXD, ssNMR and TD-NMR measurements.

	Impact of starch botanical origin	Impact of gluten addition and 5% increase in hydration level	Interpretation
To and Tp (°C)	Higher for TS-based matrices	Decrease for WS No impact for TS	Lower amylose/amylopectin ratio and level of damaged starch, and tighter crystallite organization of TS45, weaker organization of WS (thicker amorphous lamella) and decrease with rise in accessible water
ΔH 1 (J/g)	Higher for WS-based matrices	Increase for both TS and WS	Higher dissolution of amorphous regions and DH dissociations for WS. Positive impact of water increase on dissolution of amorphous regions.
RC% loss	Higher crystallite melting for TS and equal melting in model dough systems	Inhibition of crystallite melting for TS and no impact on WS	Higher crystallite melting and a hindrance effect of gluten addition on the melting of TS crystals
DH% loss	No impact of DH dissociation for starch model systems Higher DH dissociation for WSG50 compared to TSG50	Inhibition of DH dissociation for both TS and WS	Higher order loss for WS. In model dough systems, hindrance effect of gluten on both WS and TS
SPH% loss	Higher increase in mobility for WS-based systems	Inhibition of increase in mobility for WS and no impact on TS	Higher increase in mobility for WS-based matrices compared to TS (tighter organization in TS systems). Hindrance effect of gluten on starch gelatinization in WS-based matrices

increase in water-starch interactions. Relatively lower RC% loss can be attributed to the lower sensitivity of WAXD technique to molecular dynamics occurring at the molecular scale.

From 20 to 85 °C (20–75 °C in case of DH% loss), still a high correlation between DH% and SPH% loss was observed while RC% loss was lower that these two values in general. This observation can provide more evidence for differences in sensitivity of these techniques and multi-step nature of hydrothermal changes in starch.

As it is shown in Table 5, majority of techniques implemented in this work could confirm the hindrance effect of gluten on starch gelatinization and among proposed assumptions, the role of starch botanical origin can be highlighted.

5. Conclusion

The multi-scale investigation of heat-induced transformation of starch (tapioca *versus* wheat) in model dough systems compared to their pure starch counterparts highlights the importance of taking the botanical origin, hydration level, and gluten hindrance effect into account when analyzing complex matrices such as bread dough. Results showed that, at intermediate hydration levels, water ingress into starch granules, increase in glucan chain mobility and DH dissociation occurred at lower temperatures than did melting of crystallites. Moreover, by conducting our quantitative analysis using VT TD-NMR for the solid and liquid phases (SPH%), VT ssNMR for changes in DH dissociation (DH%), and VT WAXD for relative crystallinity (RC%) loss, we were able to provide evidence concerning the inhibitory effect of gluten on hydrothermal changes in starch, a topic of some controversy in the literature.

With the benefit of the T2 assignments proposed for starch-water, and gluten-water systems in our previous work, we refined the assignments for the model dough systems. The evolution of T2 parameters during the heat-induced transformation of the model dough systems more closely matched that in their starch-water system counterparts (consistent with the literature), contributing to the discussion on the degree to which starch origin determines these differences. We assessed the effects of the addition of gluten to the starch-water system using T2 mass intensity evolutions, highlighting a hindrance effect of gluten on the water-starch interactions, at least for wheat starch. Although the competition for water between gluten and starch has already been mentioned in the literature, to our knowledge, no NMR study has previously succeeded in providing quantitative evidence for this. The investigations carried out here can be continued by building up more complex systems at different hydration levels accompanied by complementary measurements (techniques discussed above) to gain a better understanding of the water distribution and hydrothermal changes of starch and gluten during real dough transformation.

This study has also provided additional evidence concerning the

sensitivity and detection scales of the different techniques at 50% water content. Correlation tests showed a good relationship between ssNMR and TD-NMR techniques. It was demonstrated that the botanical origin of the starch significantly affects the temperature range within which gelatinization occurs, as well as the extent of gelatinization at equivalent hydration levels. Further, the addition of gluten was found to influence the extent of double helix loss and to increase both the mobility of starch chains and crystallinity loss.

CRediT authorship contribution statement

Elham Rakhshi: Formal analysis, Investigation, Methodology, Project administration, Writing – original draft. **Xavier Falourd:** Methodology. **Ruud Adel Den:** Methodology. **John van Duynhoven:** Validation. **Tiphaine Lucas:** Funding acquisition, Methodology, Validation, Writing – original draft. **Corinne Rondeau-Mouro:** Funding acquisition, Methodology, Project administration, Supervision, Validation, Writing – review & editing.

Declaration of competing interest

The authors declare that they have no known competing financial interests or personal relationships that could have appeared to influence the work reported in this paper.

Data availability

The data that has been used is confidential.

Appendix A. Supplementary data

Supplementary data to this article can be found online at https://doi.org/10.1016/j.foodhyd.2023.109616.

References

Acri, G., Sansotta, C., Ruello, E. V., Denaro, L., Salmeri, F. M., & Testagrossa, B. (2021). The use of time domain NMR in food analysis : A review. *Current Nutrition & Food Science, 17*(6), 558–565. https://doi.org/10.2174/1573401316999201126212143

Atichokudomchai, N., Varavinit, S., & Chinachoti, P. (2004). A study of ordered structure in acid-modified tapioca starch by C CP/MAS solid-state NMR. *Carbohydrate Polymers, 58*(4), 383–389. https://doi.org/10.1016/j.carbpol.2004.07.017

Baks, T., Bruins, M. E., Janssen, A. E. M., & Boom, R. M. (2008). Effect of pressure and temperature on the gelatinization of starch at various starch concentrations. *Biomacromolecules, 9*(1), 296–304. https://doi.org/10.1021/bm700814a

BeMiller, J. N. (2011). Pasting, paste, and gel properties of starch–hydrocolloid combinations. *Carbohydrate Polymers, 86*(2), 386–423. https://doi.org/10.1016/j.carbpol.2011.05.064

Bertoft, E. (2017). Understanding starch structure : Recent progress. *Agronomy, 7*(3), 56. https://doi.org/10.3390/agronomy7030056

Biliaderis, C. G., Maurice, T. J., & Vose, J. R. (1980). Starch gelatinization phenomena studied by differential scanning calorimetry. *Journal of Food Science, 45*(6), 1669–1674. https://doi.org/10.1111/j.1365-2621.1980.tb07586.x

Bosmans, G. M., Lagrain, B., Deleu, L. J., Fierens, E., Hills, B. P., & Delcour, J. A. (2012). Assignments of proton populations in dough and bread using NMR relaxometry of starch, gluten, and flour model systems. *Journal of Agricultural and Food Chemistry, 60*(21). https://doi.org/10.1021/jf3008508. Article 21.

Cooke, D., & Gidley, M. J. (1992). Loss of crystalline and molecular order during starch gelatinisation : Origin of the enthalpic transition. *Carbohydrate Research, 227*, 103–112. https://doi.org/10.1016/0008-6215(92)85063-6

Debet, M. R., & Gidley, M. J. (2006). Three classes of starch granule swelling : Influence of surface proteins and lipids. *Carbohydrate Polymers, 64*(3), 452–465. https://doi.org/10.1016/j.carbpol.2005.12.011

Debet, M. R., & Gidley, M. J. (2007). Why do gelatinized starch granules not dissolve completely? Roles for amylose, protein, and lipid in granule "ghost" integrity. *Journal of Agricultural and Food Chemistry, 55*(12), 4752–4760. https://doi.org/10.1021/jf070004o

Dome, K., Podgorbunskikh, E., Bychkov, A., & Lomovsky, O. (2020). Changes in the crystallinity degree of starch having different types of crystal structure after mechanical pretreatment. *Polymers, 12*(3), 641. https://doi.org/10.3390/polym12030641

Doona, C. J., & Baik, M.-Y. (2007). Molecular mobility in model dough systems studied by time-domain nuclear magnetic resonance spectroscopy. *Journal of Cereal Science, 45*(3), 257–262. https://doi.org/10.1016/j.jcs.2006.07.015

Eliasson, A.-C. (1980). Effect of water content on the gelatinization of wheat starch. *Starch - Stärke, 32*(8), 270–272. https://doi.org/10.1002/star.19800320806

Eliasson, A.-C. (1983). Differential scanning calorimetry studies on wheat starch—gluten mixtures. *Journal of Cereal Science, 1*(3), 199–205. https://doi.org/10.1016/S0733-5210(83)80021-6

Eliasson, A.-C., & Larsson, K. (1993). *Cereals in breadmaking : A molecular colloidal approach (1re éd.)*. Marcel Dekker, Inc. https://doi.org/10.1201/9781315139005

Frost, K., Kaminski, D., Kirwan, G., Lascaris, E., & Shanks, R. (2009). Crystallinity and structure of starch using wide angle X-ray scattering. *Carbohydrate Polymers, 78*(3), 543–548. https://doi.org/10.1016/j.carbpol.2009.05.018

Gao, X., Tong, J., Guo, L., Yu, L., Li, S., Yang, B., et al. (2020). Influence of gluten and starch granules interactions on dough mixing properties in wheat (Triticum aestivum L.). *Food Hydrocolloids, 106*, Article 105885. https://doi.org/10.1016/j.foodhyd.2020.105885

Grenier, D., Rondeau-Mouro, C., Dedey, K. B., Morel, M.-H., & Lucas, T. (2021). Gas cell opening in bread dough during baking. *Trends in Food Science & Technology, 109*, 482–498. https://doi.org/10.1016/j.tifs.2021.01.032

Hibbard, P. L. (1895). Quick estimation of starch. *Journal of the American Chemical Society, 17*(1), 64–68. https://doi.org/10.1021/ja02156a010

Huang, J., Wang, Z., Fan, L., & Ma, S. (2022). A review of wheat starch analyses : Methods, techniques, structure and function. *International Journal of Biological Macromolecules, 203*, 130–142. https://doi.org/10.1016/j.ijbiomac.2022.01.149

Jekle, M., Mühlberger, K., & Becker, T. (2016). Starch–gluten interactions during gelatinization and its functionality in dough like model systems. *Food Hydrocolloids, 54*, 196–201. https://doi.org/10.1016/j.foodhyd.2015.10.005

Jenkins, P. J., & Donald, A. M. (1998). Gelatinisation of starch : A combined SAXS/WAXS/DSC and SANS study. *Carbohydrate Research, 308*(1–2), 133–147. https://doi.org/10.1016/S0008-6215(98)00079-2

Kalichevsky, M. T., Jaroszkiewicz, E. M., Ablett, S., Blanshard, J. M. V., & Lillford, P. J. (1992). The glass transition of amylopectin measured by DSC, DMTA and NMR. *Carbohydrate Polymers, 18*(2), 77–88. https://doi.org/10.1016/0144-8617(92)90129-E

Kovrlija, R., Goubin, E., & Rondeau-Mouro, C. (2020). TD-NMR studies of starches from different botanical origins : Hydrothermal and storage effects. *Food Chemistry, 308*, Article 125675. https://doi.org/10.1016/j.foodchem.2019.125675

Kovrlija, R., & Rondeau-Mouro, C. (2017a). Hydrothermal changes of starch monitored by combined NMR and DSC methods. *Food and Bioprocess Technology, 10*(3), 445–461. https://doi.org/10.1007/s11947-016-1832-9

Kovrlija, R., & Rondeau-Mouro, C. (2017b). Multi-scale NMR and MRI approaches to characterize starchy products. *Food Chemistry, 236*, 2–14. https://doi.org/10.1016/j.foodchem.2017.03.056

Kuang, Q., Xu, J., Liang, Y., Xie, F., Tian, F., Zhou, S., et al. (2017). Lamellar structure change of waxy corn starch during gelatinization by time-resolved synchrotron SAXS. *Food Hydrocolloids, 62*, 43–48. https://doi.org/10.1016/j.foodhyd.2016.07.024

Lagrain, B., Wilderjans, E., Glorieux, C., & Delcour, J. A. (2012). Importance of gluten and starch for structural and Textural properties of crumb from fresh and stored bread. *Food Biophysics, 7*(2), 173–181. https://doi.org/10.1007/s11483-012-9255-2

Lelièvre, J., & Liu, H. (1994). A review of thermal analysis studies of starch gelatinization. *Thermochimica Acta, 246*(2), 309–315. https://doi.org/10.1016/0040-6031(94)80098-7

Leon, A., Rosell, C. M., & Benedito de Barber, C. (2003). A differential scanning calorimetry study of wheat proteins. *European Food Research and Technology, 217*(1), 13–16. https://doi.org/10.1007/s00217-003-0699-y

Martin, C., Morel, M.-H., Reau, A., & Cuq, B. (2019). Kinetics of gluten protein-insolubilisation during pasta processing : Decoupling between time- and temperature-dependent effects. *Journal of Cereal Science, 88*, 103–109. https://doi.org/10.1016/j.jcs.2019.05.014

Milde, L. B., Ramallo, L. A., & Puppo, M. C. (2012). Gluten-free bread based on tapioca starch : Texture and sensory studies. *Food and Bioprocess Technology, 5*(3), 888–896. https://doi.org/10.1007/s11947-010-0381-x

Mills, E. N. C., Wilde, P. J., Salt, L. J., & Skeggs, P. (2003). Bubble formation and stabilization in bread dough. *Food and Bioproducts Processing, 81*(3), 189–193. https://doi.org/10.1205/096030803322437956

Morel, M.-H., Redl, A., & Guilbert, S. (2002). Mechanism of heat and shear mediated aggregation of wheat gluten protein upon mixing. *Biomacromolecules, 3*(3), 488–497. https://doi.org/10.1021/bm015639p

Mutungi, C., Passauer, L., Onyango, C., Jaros, D., & Rohm, H. (2012). Debranched cassava starch crystallinity determination by Raman spectroscopy : Correlation of features in Raman spectra with X-ray diffraction and 13C CP/MAS NMR spectroscopy. *Carbohydrate Polymers, 87*(1), 598–606. https://doi.org/10.1016/j.carbpol.2011.08.032

Nara, S., Mori, A., & Komiya, T. (1978). Study on relative crystallinity of moist potato starch. *Starch - Stärke, 30*(4), 111–114. https://doi.org/10.1002/star.19780300403

Nivelle, M. A., Beghin, A. S., Bosmans, G. M., & Delcour, J. A. (2019). Molecular dynamics of starch and water during bread making monitored with temperature-controlled time domain 1H NMR. *Food Research International, 119*, 675–682. https://doi.org/10.1016/j.foodres.2018.10.045

Paris, M., Bizot, H., Emery, J., Buzare, J. Y., & Buleon, A. (1999). Crystallinity and structuring role of water in native and recrystallized starches by 13C CP-MAS NMR spectroscopy 1 : Spectral decomposition. *Carbohydrate Polymers, 39*, 327–339. https://doi.org/10.1016/S0144-8617(99)00022-3

Paris, M., Bizot, H., Emery, J., Buzaré, J. Y., & Buléon, A. (2001). NMR local range investigations in amorphous starchy substrates I. Structural heterogeneity probed by 13C CP–MAS NMR. *International Journal of Biological Macromolecules, 29*(2), 127–136. https://doi.org/10.1016/S0141-8130(01)00160-X

Raiford, D. S., Fisk, C. L., & Becker, E. D. (1979). Calibration of methanol and ethylene glycol nuclear magnetic resonance thermometers. *Analytical Chemistry, 51*(12), 2050–2051. https://doi.org/10.1021/ac50048a040

Rakhshi, E., Cambert, M., Diascorn, Y., Lucas, T., & Rondeau-Mouro, C. (2022). An insight into tapioca and wheat starch gelatinization mechanisms using TD-NMR and complementary techniques. *Magnetic Resonance in Chemistry, 60*, 702–718. https://doi.org/10.1002/mrc.5258

Ratnayake, W. S., & Jackson, D. S. (2007). A new insight into the gelatinization process of native starches. *Carbohydrate Polymers, 67*(4), 511–529. https://doi.org/10.1016/j.carbpol.2006.06.025

Riley, I. M., Nivelle, M. A., Ooms, N., & Delcour, J. A. (2022). The use of time domain [1] H NMR to study proton dynamics in starch-rich foods : A review. *Comprehensive Reviews in Food Science and Food Safety, 21*(6), 4738–4775. https://doi.org/10.1111/1541-4337.13029

Roman-Gutierrez, A. D., Guilbert, S., & Cuq, B. (2002). Distribution of water between wheat flour components : A dynamic water vapour adsorption study. *Journal of Cereal Science, 36*(3), 347–355. https://doi.org/10.1006/jcrs.2002.0470

Rondeau-Mouro, C., Cambert, M., Kovrlija, R., Musse, M., Lucas, T., & Mariette, F. (2015). Temperature-associated proton dynamics in wheat starch-based model systems and wheat flour dough evaluated by NMR. *Food and Bioprocess Technology, 8*(4), 777–790. https://doi.org/10.1007/s11947-014-1445-0

Schirmer, M., Zeller, J., Krause, D., Jekle, M., & Becker, T. (2014). In situ monitoring of starch gelatinization with limited water content using confocal laser scanning microscopy. *European Food Research and Technology, 239*(2), 247–257. https://doi.org/10.1007/s00217-014-2213-0

Shevkani, K., Singh, N., Bajaj, R., & Kaur, A. (2017). Wheat starch production, structure, functionality and applications-a review. *International Journal of Food Science and Technology, 52*(1), 38–58. https://doi.org/10.1111/ijfs.13266

Singh, V., Ali, S. Z., Somashekar, R., & Mukherjee, P. S. (2006). Nature of crystallinity in native and acid modified starches. *International Journal of Food Properties, 9*(4), 845–854. https://doi.org/10.1080/10942910600698922

Tan, I., Flanagan, B. M., Halley, P. J., Whittaker, A. K., & Gidley, M. J. (2007). A method for estimating the nature and relative proportions of amorphous, single, and double-helical components in starch granules by [13] C CP/MAS NMR. *Biomacromolecules, 8*(3), 885–891. https://doi.org/10.1021/bm060988a

Vamadevan, V., & Bertoft, E. (2015). Structure-function relationships of starch components. *Starch - Stärke, 67*(1–2), 55–68. https://doi.org/10.1002/star.201400188

Vamadevan, V., & Bertoft, E. (2020). Observations on the impact of amylopectin and amylose structure on the swelling of starch granules. *Food Hydrocolloids, 103*, Article 105663. https://doi.org/10.1016/j.foodhyd.2020.105663

Vermeylen, R., Derycke, V., Delcour, J. A., Goderis, B., Reynaers, H., & Koch, M. H. J. (2006). Structural transformations during gelatinization of starches in limited water : Combined wide- and small-angle X-ray scattering study. *Biomacromolecules, 7*(4), 1231–1238. https://doi.org/10.1021/bm050651t

Wagner, M., Morel, M.-H., Bonicel, J., & Cuq, B. (2011). Mechanisms of heat-mediated aggregation of wheat gluten protein upon pasta processing. *Journal of Agricultural and Food Chemistry, 59*(7), 3146–3154. https://doi.org/10.1021/jf104341w

Waigh, T. A., Gidley, M. J., Komanshek, B. U., & Donald, A. M. (2000). The phase transformations in starch during gelatinisation : A liquid crystalline approach.

Carbohydrate Research, 328(2), 165–176. https://doi.org/10.1016/S0008-6215(00)00098-7

Wang, S., & Copeland, L. (2013). Molecular disassembly of starch granules during gelatinization and its effect on starch digestibility : A review. *Food & Function, 4*(11), 1564. https://doi.org/10.1039/c3fo60258c

Wang, S., Li, C., Yu, J., Copeland, L., & Wang, S. (2014). Phase transition and swelling behaviour of different starch granules over a wide range of water content. *LWT - Food Science and Technology, 59*(2), 597–604. https://doi.org/10.1016/j.lwt.2014.06.028

Wieser, H. (2007). Chemistry of gluten proteins. *Food Microbiology, 24*(2), 115–119. https://doi.org/10.1016/j.fm.2006.07.004

Yang, T., Wang, P., Zhou, Q., Zhong, Y., Wang, X., Cai, J., et al. (2022). Effects of different gluten proteins on starch's structural and physicochemical properties

during heating and their molecular interactions. *International Journal of Molecular Sciences, 23*(15), 8523. https://doi.org/10.3390/ijms23158523

Zhang, Y., Junejo, S. A., Zhang, B., Fu, X., & Huang, Q. (2022). Multi-scale structures and physicochemical properties of waxy starches from different botanical origins. *International Journal of Biological Macromolecules, 220*, 692–702. https://doi.org/10.1016/j.ijbiomac.2022.08.133

Zhong, Y., Li, Z., Qu, J., Bertoft, E., Li, M., Zhu, F., et al. (2021). Relationship between molecular structure and lamellar and crystalline structure of rice starch. *Carbohydrate Polymers, 258*, Article 117616. https://doi.org/10.1016/j.carbpol.2021.117616

Petrofsky, K.E., & Hoseney, R.C. (1995). Rheological properties of dough made with starch and gluten from several cereal sources'. Cereal Chemistry, 72(l), 53-58.